Spectroscopic ellipsometry and Raman study of fluorinated nanocrystalline carbon thin films

Hosun Lee[a] and In-Young Kim
Department of Physics and Institute for Natural Sciences, Kyung Hee University, Suwon 449-701, South Korea

S.-S. Han[b] and B.-S. Bae
Department of Material Science and Engineering, Laboratory of Optical Materials and Coating, Korea Advanced Institute of Science and Technology, Taejon 305-701, South Korea

M. K. Choi and In-Sang Yang
Department of Physics, Ewha Womans University, Seoul 120-750, South Korea

(Received 2 January 2001; accepted for publication 16 April 2001)

Using spectroscopic ellipsometry and Raman spectroscopy, we measured the pseudodielectric function and the phonon frequencies of fluorinated nanocrystalline carbon (nc-C:F) thin films grown on silicon substrate at varying growth temperature and gas flux ratio of CH_4 and CF_4. Utilizing the Tauc–Lorentzian formula, we performed multilayer analysis to estimate the dielectric function of the fluorinated nanocrystalline carbon thin films. We also adopted Gaussian-like density-of-states model proposed by Demichelis *et al.* [Phys. Rev. B **45**, 14364 (1992)] and estimated the amplitude A, the transition energy E_π, and the broadening σ_π of $\pi \rightarrow \pi^*$ transitions. Based on this model, we explained the change of the optical gap and the refractive index in terms of the change of the amplitude A rather than the shift of transition energy E_π of $\pi \rightarrow \pi^*$ transitions. Raman and ellipsometric study suggested that the average size of nanocrystallites in the fluorinated carbon thin films was smaller than that of amorphous hydrogenated carbon films studied by Hong *et al.* [Thin Solid Films **352**, 41 (1999)]. © *2001 American Institute of Physics.* [DOI: 10.1063/1.1378337]

I. INTRODUCTION

Diamond-like carbon films are intensively investigated in various forms such as amorphous carbon (a-C), hydrogenated amorphous carbon (a-C:H), or fluorinated amorphous carbon(a-C:F). The structure of carbon films can be classified as polymer-like, diamond-like, or graphite-like. The electronic and optical properties of carbon films are closely related to the ratio of sp^2 and sp^3 hybridized bonds.[1,2] Refractive indexes in the visible range are determined mainly by the strength of transitions between π and π^* states which are related to sp^2 hybridized bonds. Ellipsometric study of various types of nanocarbon films was reported by Collins and co-workers.[3,4] Recently Hong *et al.* measured the pseudodielectric function and phonon frequencies of a-C:H grown on silicon substrate using spectroscopic ellipsometry and Raman spectroscopy.[5] Adopting Gaussian-like density-of-states (DOS) model proposed by Demichellis *et al.*, they estimated the complex refractive indexes of a-C:H films.[6] With increasing H content, they observed a decrease of refractive indexes. Thin films of fluorinated amorphous carbon ($a-$C:F) layer can be utilized for intermetal dielectric material in ultralarge scale integration circuits to isolate the metal lines.[7–9] This application requires the lowest dielectric constant materials to reduce the parasitic capacitance between metal lines. So far, no ellipsometric and Raman study for $a-$C:F has been performed to investigate the effect of gas flow ratio and thermal annealing on the refractive indexes. And it is very important to investigate the optical effect of the addition of fluorine instead of hydrogen into amorphous carbon.

Here we measured the pseudodielectric function and phonon frequencies of fluorinated nanocrystalline carbon (nc-C:F) thin films grown on a silicon substrate at varying growth temperatures and gas flow ratio of CH_4 and CF_4 using spectroscopic ellipsometry and Raman spectroscopy. Utilizing the Tauc–Lorentzian formula, we performed multilayer analysis to estimate the dielectric function ($n+ik=\sqrt{\epsilon}$) of fluorinated nanocrystalline carbon thin films.[10] We determined phenomenological optical gap such as E_{04}. We also adopted the Gaussian-DOS model and estimated the transition energy E_π of $\pi \rightarrow \pi^*$ transitions. Based on this model, we explained the change of the transition energy and the refractive indexes in nc-C:F thin films. We also compared our result to that of a-C:H thin films reported in the literature. (Note: Raman data of high-temperature-annealed fluorinated carbon films suggested that they had the characteristic of nanocrystalline graphite rather than that of amorphous carbon. Hence we designate the films as nc-C:F rather than a-C:F.)

[a]Author to whom correspondence should be addressed; electronic mail: hlee@khu.ac.kr
[b]Present address: LG-Philips LCD Inc., Anyang 431-080, South Korea.

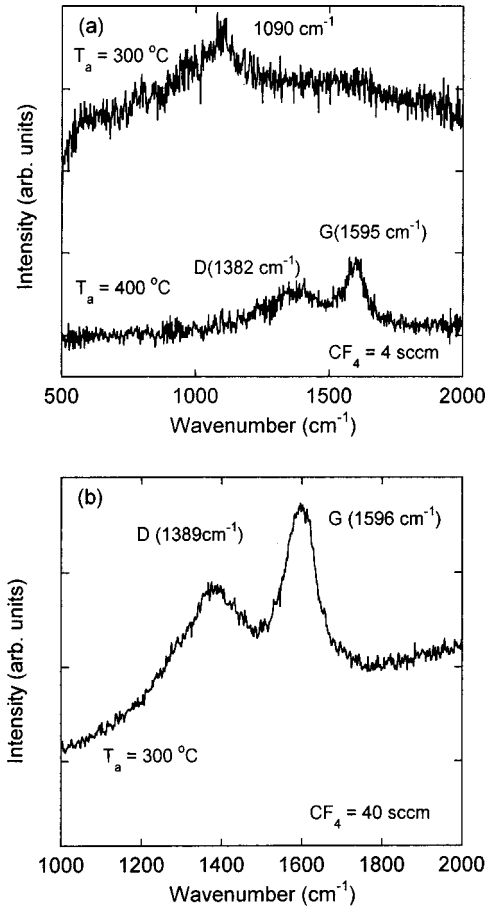

FIG. 1. Plot of Raman spectra measured using the 5145 Å line of an argon ion laser of annealed nc-C:F thin films grown with CF_4 flow rate of: (a) 4 sccm and (b) 40 sccm.

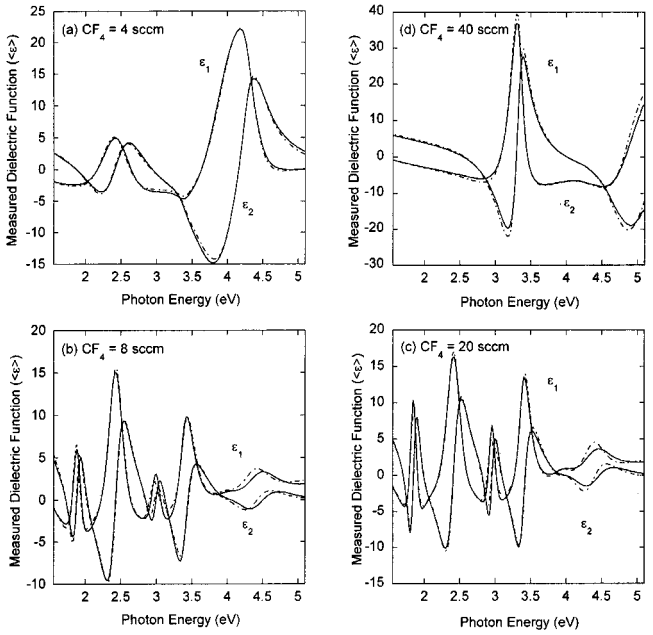

FIG. 2. Plot of the pseudodielectric function $[\epsilon=\epsilon_1+i\epsilon_2]$ (solid line) of nc-C:F grown on Si substrate for flow rate of $[CH_4=4$ sccm, $CF_4=$(a) 4, (b) 8, (c) 20, and (d) 40 sccm] and its curve fit (dot-dashed line) using the Tauc–Lorentzian formula.

II. EXPERIMENTS

We grew nc-C:F thin films at room temperature by inductively coupled-plasma chemical vapor deposition system. The thin films were deposited on (100) *p*-type Si substrates using CH_4/CF_4 as reactant gases, and Ar as a diluent gas. We grew samples with a varying $CH_4:CF_4$ flow rate ratio and annealed them at various temperatures to obtain a stable phase. While the CH_4 flow rate was constant at 4 sccm, the CF_4 flow rate was increased from 4 to 40 sccm.[8] Samples were annealed under vacuum (10^{-2} Torr) for 30 min at various temperatures (100, 200, 300, and 400 °C).[9] The compositions of C, F, and H were estimated quantitatively using the elastic recoil detection–time-of-flight method. For example, the compositions were determined to be about 70%, 25%, and 5%, respectively, for 4 sccm of CH_4 and CF_4 flow rate. With increasing CF_4 flow rate, the F content increased slightly by 2%–3%. With increasing annealing temperature, the F content decreased down to 15% at 400 °C. The H content also decreased to a negligible content with increasing annealing temperature.[8]

We measured the pseudodielectric function of samples using rotating-analyzer-type spectroscopic ellipsometer with autoretarder (VASE model, J. A. Woollam Company). The angle of incidence was fixed at 70° and the spectral range was from 1.2 to 5.2 eV. Samples were characterized using Raman spectroscopy in a backscattered geometry at room temperature using a subtractive triple spectrometer with a charge coupled detector at an excitation wavelength of 5145 Å. We used a low power laser beam of 3 mW into the area of 100 μm^2 to avoid unwanted annealing during Raman measurement.

III. RESULTS AND DISCUSSION

Figure 1 is the plot of Raman spectra which were measured using the excitation wavelength of 5145 Å of an argon-ion laser. Characteristic phonons near 1090 cm^{-1}, 1385 cm^{-1} (*D* peak), and 1595 cm^{-1} (*G* peak) were discernible only in the samples annealed above 300 °C. Raman spectra of the samples annealed at lower temperature were dominated by a strong and broad fluorescence peak. Each phonon peak was fitted using Gaussian line shape fitting. According to the literature, 1090 cm^{-1} peak is correlated with sp^3 bond content, *D* peak arises only from clusters of sp^2 sites in sixfold aromatic rings, and *G* peak arises from vibrations of all sp^2 sites (in both chain and ring configurations).[11,12]

Raman spectra of *a*-C:H with about 30% of H were measured by Hong *et al.*[5], and *D* and *G* peaks were observed at lower wave numbers at 1355 and 1570 cm^{-1}. Ferrari and Robertson interpreted that the increase in *G* peak frequency is due to the formation of the nanocrystalline graphite phase.[13] Thus nc-C:F should have a more nanocrystalline phase or smaller size of nanocrystalline graphites than that of *a*-C:H for the same concentration of F or H atoms.

Figure 2 is the plot of pseudodielectric function spectra of nc-C:F grown on a Si substrate with varying $CH_4:CF_4$ flux ratio [(a) 4:4, (b) 4:8, (c) 4:20, and (d) 4:40]. Solid lines are raw data and dot-dashed lines are fitted curves determined after multilayer analysis. We assumed three phase

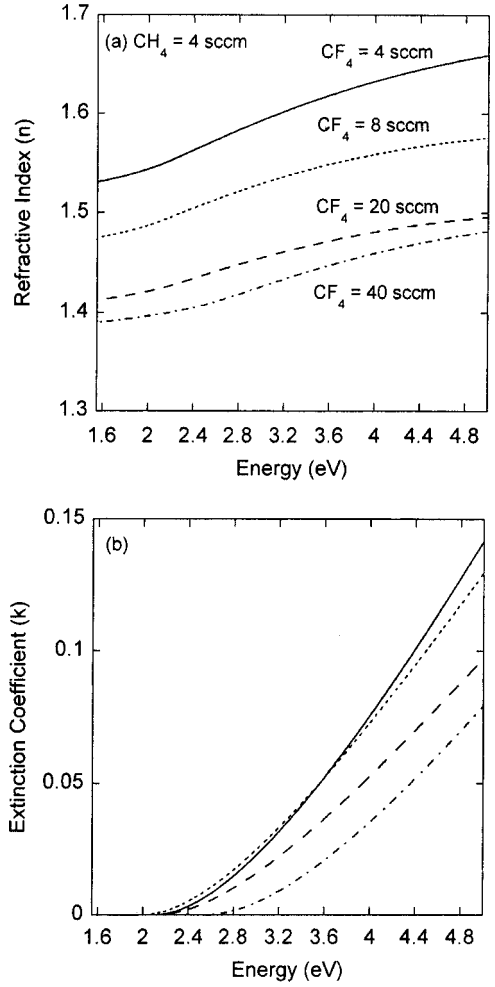

FIG. 3. Plot of (a) refractive indexes (n) and (b) extinction coefficients (k) of nc-C:F layers with different flow ratio ($CH_4=4$ sccm, $CF_4=4$, 8, 20, and 40 sccm).

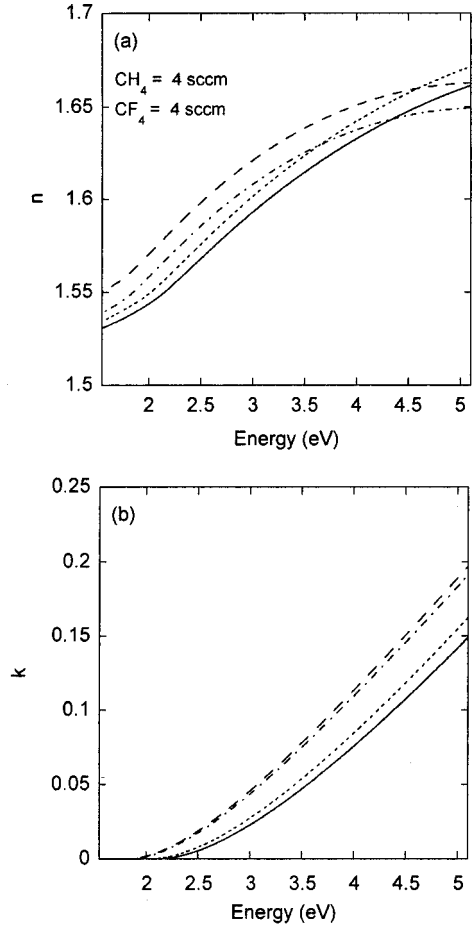

FIG. 4. Plot of (a) refractive indexes (n) and (b) extinction coefficients (k) of nc-C:F layers at fixed flowing rate ($CH_4=CF_4=4$ sccm) with varying annealing temperature (solid line: as-grown, dotted line: 100 °C, dashed line: 200 °C, dot-dashed line: 300 °C).

model (air–nc-C:F–Si substrate) and adopted the Tauc–Lorentzian model to estimate the dielectric function of the nc-C:F layer. The dielectric function values of bulk Si were quoted from the literature.[14] The fitting procedure uses a nonlinear regression method based on the Levenberg–Marquardt algorithm.[15] More detailed modeling, for example, multilayer analysis including the roughness layer on the surface did not improve the fitting.

The Tauc–Lorentzian model is a parametrization method of optical function of nanocrystalline semiconductors in which the imaginary dielectric function ϵ_2 is determined by multiplying the Tauc joint density of states by the ϵ_2 obtained from the Lorentz oscillator model.[10] Thus the imaginary part of the dielectric function ϵ_2 is given by

$$\epsilon_2(E)=\frac{1}{E}\left[\frac{AE_0C(E-E_g)^2}{(E^2-E_0^2)^2+C^2E^2}\right] \quad \text{for } E>E_g$$
$$=0 \quad \text{for } E<E_g, \tag{1}$$

where A, E, E_g, and C are the four parameters to describe the spectral dependence of $\epsilon_2(E)$. The real part of the dielectric function $\epsilon_1(E)$ is then obtained in a closed form through Kramers–Kronig transformation, with an additional parameter $\epsilon_{1\infty}$.

Figure 3 is the plot of (a) refractive indexes (n) and (b) extinction coefficients (k) of nc-C:F layers, which were fitted with multilayer analysis using the Tauc–Lorentzian model. With more fluorine content, it appeared that refractive indexes decreased as expected. Figure 4 is the plot of fitted complex refractive indexes ($n+ik$) of as-grown and annealed nc-C:F layers as a function of annealing temperature for the fixed flow rate of 4 sccm of CH_4 and CF_4 flux. With increasing annealing temperature, the refractive indexes appeared to increase in general because H and F content decreased. We note that separate H or F aggregates of atoms do not contribute to the dielectric function in the visible range. Figure 5(a) is the E_{04} gap with increasing CF_4 flow rate at fixed $CH_4=4$ sccm and Fig. 5(b) is the same plot with increasing annealing temperature for the fixed flow rate of 4 sccm of CH_4 and CF_4. The E_{04} gap is defined as the energy value where the absorption is equal to 10^{-4}cm^{-1}. The optical gap increased with increasing CF_4 flow rate because the refractive index decreased due to the increase of F composition in nc-C:F thin films. The optical gap decreased as the

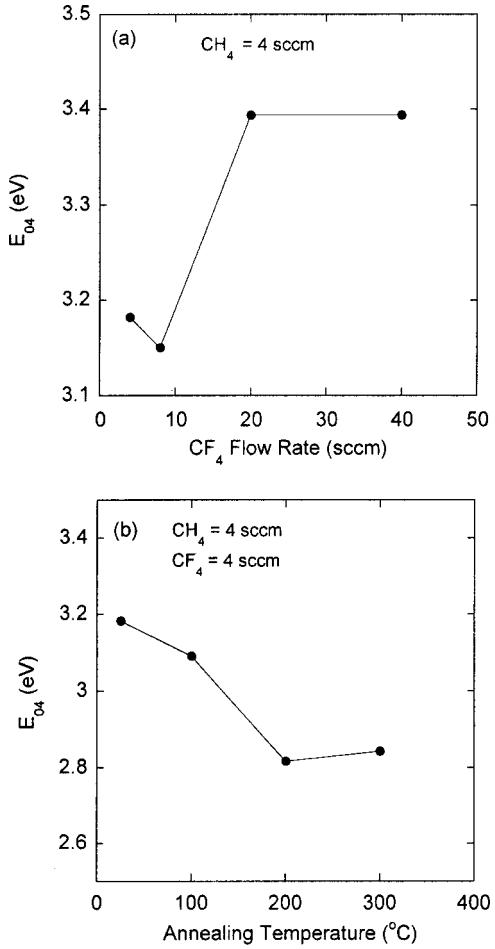

FIG. 5. Plot of optical gap E_{04} for (a) varying CH_4 and CF_4 flow ratio and for (b) annealing temperature at fixed flow ratio of 4 sccm for both CH_4 and CF_4 flow.

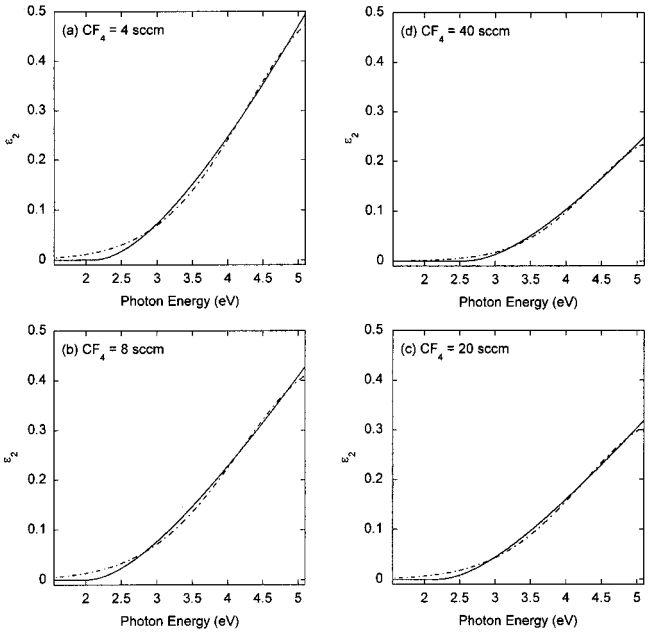

FIG. 6. Plot of imaginary dielectric function ϵ_2 of nc-C:F layer [$CH_4=4$ sccm, $CF_4=$(a) 4, (b) 8, (c) 20, and (d) 40 sccm] converted from the refractive index values in Fig. 3 (solid line) and its curve fit using Gaussian density of states model (dot-dashed line).

annealing temperature increased as expected because H and F content decreased.

The layer of nc-C:F is supposed to be composed of graphitic islands embedded in a matrix of diamond-like phase similar to the *a*-C:H layer. The bands of nc-C:F can be considered a weighted average of the bands of two phases. However, no contribution from the diamond phase is expected for energies near the Fermi energy. In the graphitic islands, the ''valence'' band is formed by a σ band (well below the Fermi level) and a π band (near the Fermi level). Symmetrically, the ''conduction'' band is formed by a π^* band (near the Fermi level) and a σ^* band (well above the Fermi level).[1,6] For low photon energies ($\leqslant 5$ eV), absorption takes place mainly in the graphitic islands through $\pi-\pi^*$ transitions. Other transition energies of $\sigma-\pi^*$, $\pi-\sigma^*$, and $\sigma-\sigma^*$ are too high and are out of our spectral range between 1.2 and 5.2 eV. We adopted the Gaussian-like DOS model, symmetrical with respect to the Fermi level between π and π^* bands, which is given by

$$\epsilon_2(E)=\frac{A}{E^2}\,\mathrm{erf}\left(\frac{E}{2\sigma_\pi}\right)\exp\left(-\left(\frac{2E_\pi-E}{2\sigma_\pi}\right)^2\right), \qquad (2)$$

where fitted parameters are the amplitude A, energy E_π, and width σ_π of the Gaussian distribution function in $\pi\rightarrow\pi^*$ transitions.[6]

Figures 6(a)–6(d) are the imaginary dielectric function values of the nc-C:F layer which were converted from the refractive index values of the nc-C:F layer in Fig. 3 and their Gaussian DOS fit with varying flow ratio ($CH_4=4$ sccm, $CF_4=4$, 8, 20, and 40 sccm). The Gaussian DOS fit is not as good below 3 eV probably due to the band tail of Gaussian DOS bands in $\pi-\pi^*$ transitions. This kind of band tail is similar to the case of *a*-C:H. We only needed $\pi-\pi^*$ transitions to fit the ϵ_2 spectra for nc-C:F in our spectral range because the transition energy E_σ associated with $\sigma-\sigma^*$ transitions was too high. According to Hong *et al.*, E_σ (E_0 in their notation) of *a*-C:H was low enough that E_σ could be fitted from the low energy tails of the E_σ peak between 4 and 5 eV from the ϵ_2 spectra.

Figure 7 is the plot of amplitude, transition energy, and broadening of $\pi\rightarrow\pi^*$ transitions determined from Fig. 6 with increasing CF_4 flow rate at fixed $CH_4=4$ sccm. Figure 8 is the same plot with a different annealing temperature with a fixed flow ratio of $CH_4=CF_4=4$ sccm. The fitted E_π of nc-C:F was about 3 eV. This value is higher than 2.2–2.3 eV of *a*-C:H reported by Hong *et al.*[5] We did not observe any onset of $\sigma\rightarrow\sigma^*$ transitions in Fig. 6 in our spectral energy to the contrary of that of *a*-C:H thin films reported by Hong *et al.* Therefore the transition energy associated with $\sigma\rightarrow\sigma^*$ transitions should also be higher than that of *a*-C:H thin films reported by them. As shown in Fig. 1, the higher *G* peak phonon frequency of nc-C:F may also indicate that the size of the nanocrystalline graphite phase may be smaller than that of *a*-C:H. The smaller nanocrystalline graphite size

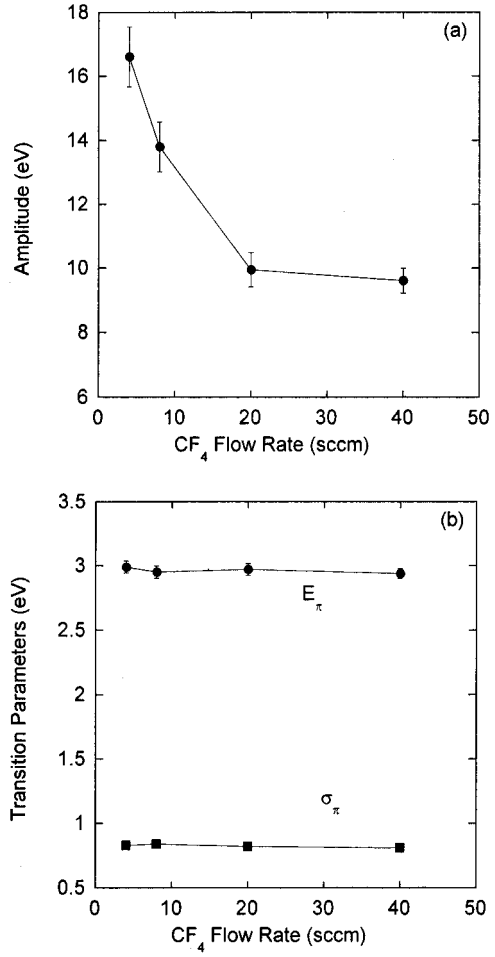

FIG. 7. Plot of (a) amplitude and (b) energy and broadening of Gaussian distribution function in $\pi-\pi^*$ transition as a function of CF_4 flow rate (fixed $CH_4=4$ sccm). The error bars designate 95% reliability.

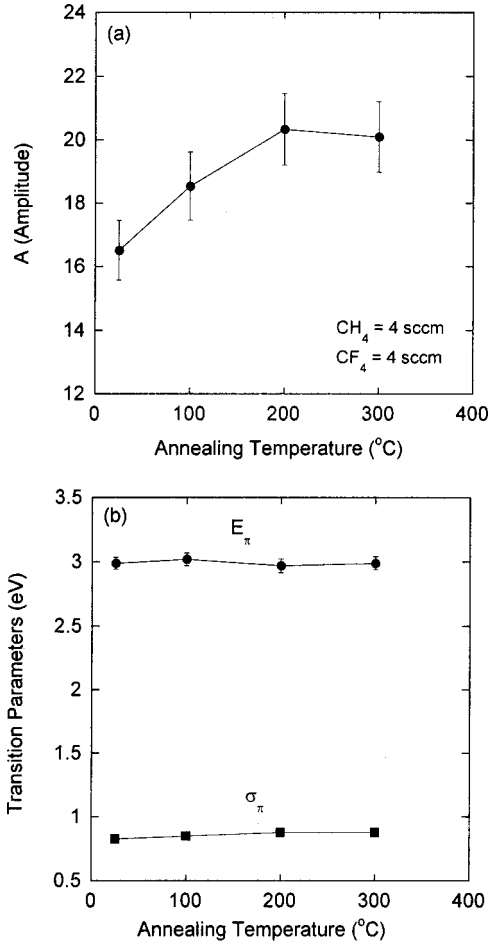

FIG. 8. The same plot as Fig. 7 as a function of annealing temperature with fixed flow ratio ($CH_4=CF_4=4$ sccm). The error bars designate 95% reliability.

should cause higher transition energies of $\pi\rightarrow\pi^*$ and $\sigma\rightarrow\sigma^*$ transitions than those of a-C:H thin films.

In Figs. 7 and 8, the amplitude decreased with more CF_4 flow and increased with increasing annealing temperature. With increasing temperature, fluorine content decreased. However, the transition energy and broadening did not change much. Thus the change of transition amplitude was the main factor of the change of refractive indexes. With increasing CF_4 flux, E_π increased slightly and σ_π was almost constant. With increasing annealing temperature, E_π was almost constant and σ_π increased slightly. The decrease of the amplitude with more fluorine content can be interpreted as the decrease of sp^2 contents.

Analysis of the dielectric function based on the Gaussian DOS model shows that the change of E_{04} gap can be caused by the change of amplitude of $\pi\rightarrow\pi^*$ transitions (the concentration of sp^2 bonds) as was suggested by Oppedisano and Tagliaferro for a-C:H.[16] We attribute the increase of the E_{04} gap to the reduction of the amplitude of $\rightarrow\pi^*$ transitions A_π with increasing fluorine content.

For fluorinated SiO_2, Han and Aydil systematically investigated the effect of fluorine on the dielectric function and concluded that the reduction of dielectric function is a combined effect of two factors: (1) the reduction of electronic and, to a lesser degree, ionic polarization due to incorporation of the Si–F bond in place of the Si–O bond and (2) creation of voids in the SiO_2 matrix, i.e., less dense, more porous film.[17] A similar phenomenon may explain the reduction of refractive indexes of nc-C:F. In terms of the Gaussian DOS model, increasing fluorine content makes the amplitude of $\pi\rightarrow\pi^*$ transitions smaller, which is caused by two factors: (1) the reduction of the amplitude of $\pi\rightarrow\pi^*$ transitions due to incorporation of the C–F bond in place of the C–C bond and (2) creation of voids in the carbon matrix and consequently, less dense and more porous film.

IV. CONCLUSION

We measured the dielectric function and the phonon frequencies of fluorinated nanocrystalline carbon (nc-C:F) thin films grown on silicon substrate using spectroscopic ellipsometry and Raman spectroscopy at varying gas flow rates of CH_4 and CF_4 and several annealing temperatures. Utilizing the Tauc–Lorentzian formula, we performed multilayer analysis to estimate the dielectric function of nc-C:F thin films. We determined optical gaps such as E_{04}. We also adopted the Gaussian-like DOS model and estimated the am-

plitude, transition energy, and broadening parameters of $\pi \rightarrow \pi^*$ transitions. Based on this model, we explained the change of complex refractive indexes and the shift of the E_{04} gap energy in terms of the change of the amplitude of $\pi \rightarrow \pi^*$ transitions, i.e., the change of concentration of sp^2 hybrid bonds. We determined that the lowest refractive indexes were achieved with the highest CF_4 gas flow rate and that thermal annealing increased the refractive indexes. Raman study suggested that the volume fraction of the nc-C:F naocrystalline phase could be more abundant or the size of nanocrystalline graphites may be smaller than that of *a*-C:H films for the same content of F or H atoms. The smaller size of nanocrystalline graphites should explain the higher value of transition energies E_π and E_σ, which are associated with $\pi \rightarrow \pi^*$ and $\sigma \rightarrow \sigma^*$ transitions in nc-C:F thin films compared to those of *a*-C:H thin films studied by Hong *et al.*[5]

ACKNOWLEDGMENT

H.L. wishes to acknowledge the financial support of the Korea Research Foundation Grant (KRF-99-015-DP0152).

[1] J. Robertson, Philos. Mag. B **76**, 335 (1997).
[2] J. Robertson, Adv. Phys. **35**, 317 (1986).
[3] Y. Cong, R. W. Collins, G. F. Epps, and H. Windischmann, Appl. Phys. Lett. **58**, 819 (1991).
[4] J. Lee, R. W. Collins, V. S. Veerasamy, and J. Robertson, Diamond Relat. Mater. **7**, 999 (1998).
[5] J. Hong, A. Goulet, and G. Turban, Thin Solid Films **352**, 41 (1999).
[6] F. Demichelis, C. F. Pirri, and A. Tagliaferro, Phys. Rev. B **45**, 14364 (1992).
[7] K. Endo, K. Shinoda, and T. Tatsumi, J. Appl. Phys. **86**, 2739 (1999).
[8] S.-S. Han, H. R. Kim, and B.-S. Bae, J. Electrochem. Soc. **146**, 3383 (1999).
[9] S.-S. Han and B.-S. Bae (unpublished).
[10] G. E. Jellison, Jr. and F. A. Modine, Appl. Phys. Lett. **69**, 371 (1996); **69**, 2137 (1996).
[11] K. W. R. Gilkes, S. Prawer, K. W. Nugent, J. Robertson, H. D. Sands, Y. Lifshitz, and X. Shi, J. Appl. Phys. **87**, 7283 (2000).
[12] M. Chhowalla, A. C. Ferrari, J. Robertson, and G. A. J. Amaratunga, Appl. Phys. Lett. **76**, 1419 (2000).
[13] A. C. Ferrari and J. Robertson, Phys. Rev. B **61**, 14095 (2000).
[14] C. M. Herzinger, B. Johs, W. A. McGahan, J. A. Woollam, and W. Paulson, J. Appl. Phys. **83**, 3323 (1998).
[15] W. H. Press, B. P. Flannery, S. A. Teukolsky, and W. T. Vetterling, *Numerical Recipes: The Art of Scientific Computing*, 2nd ed. (Cambridge University Press, New York, 1992).
[16] C. Oppedisano and A. Tagliaferro, Appl. Phys. Lett. **75**, 3650 (1999).
[17] S. M. Han and E. S. Aydil, J. Appl. Phys. **83**, 2172 (1998).